Conductance Quasi-quantization of Quantum Point Contacts: Why Tight Binding Models Are Insufficient

Stefan Kirchner[1], Johann Kroha[2], Peter Wölfle[1], and Elke Scheer[3]

[1] Institut für Theorie der Kondensierten Materie, Universität Karlsruhe, 76128 Karlsruhe, Germany
[2] Physikalisches Institut der Universität Bonn, 53115 Bonn, Germany
[3] Fachbereich Physik, Universität Konstanz, 78457 Konstanz, Germany

1 Introduction

Recent advances in miniaturization techniques have proliferated the theoretical and experimental interest in controlling transport through contacts with minimal possible size. From a purely classical point of view, where the problem resembles the one of calculating the passage of a dilute gas through a narrow hole, one obtains for the resistance R of such a point contact [1]

$$R = \frac{p_F}{e^2 D^2 n_e}, \tag{1}$$

where p_F is the Fermi momentum, n_e is the electron density and D is the diameter of the contact. This resistance is commonly referred to as the Sharvin resistance. For small contacts quantum effects will become important, since for small D only a limited number of eigenmodes of the electronic system under consideration can fit into the contact, and consequently the quantization of the transverse momentum limits the transport through the system. In the case of non-interacting electrons each transmission channel or eigenmode will carry one quantum of conductance $G_0 = 2e^2/h$, corresponding to a resistance of 12.9kΩ. The factor 2 in this formula is due to spin degeneracy. In general, the probability τ_i of channel i can be any number between zero and one characterizing the conductance of each channel in units of the quantum of conductance. The total transmission probability $\mathcal{T}$ is the sum of all single channel transmission coefficients,

$$\mathcal{T} = \sum_{i=1}^{M} \tau_i, \quad \text{with} \quad \tau_i \in [0,1], \tag{2}$$

and can be any number between zero and M, where M is the number of channels present. The total conductance is therefore given by

$$G = 2\frac{e^2}{h}\mathcal{T}. \tag{3}$$

In the linear response regime the conductance $G = \frac{dI}{dV}|_{V=0}$ is related to the local density of states (LDoS) of the interacting region provided the coupling to left and right lead is symmetric [2]. Hence, it seems sufficient to determine the number of channels M and the independent transmissions τ_i. In the following we will briefly review the experimental findings and then discuss which problems may arise in a simple tight-binding modelling of the junction. A more complete treatment of these problems leads to an interacting model. In the case of strong interactions we are able to connect the experimental findings to an approximate sum rule.

2 Experimental Observations

Experiments on a large ensemble of metallic contacts have demonstrated the *statistical* tendency of atomic-size contacts to have preferred values of conductance G [3]. The experimental evidence stems from conductance histograms calculated from repeated recordings of breaking curves from contacts fabricated by different experimental methods such as scanning tunnelling microscopes (STM) [4], dangling wires [5] or mechanically controllable breakjunctions (MCB) [6].

In the case of monovalent metals the preferred values are often close to integer multiples of G_0 [4,6,5]. The natural explanation of this finding is a set of transport channels that are either fully open ($\tau_i = 1$) or completely closed ($\tau_i = 0$), i.e. that there is an underlying "transmission quantization". This interpretation is supported by measurements of the shot noise [7], the thermo-power [8] or the conductance fluctuation amplitude [9] of gold few-atom contacts fabricated with the mechanically controllable break-junction technique. For all three properties a minimum is expected and observed when fully open transport channels are present. Here, it is thought that each individual transport channel is made up of the *single* valence orbital of a monovalent atom and that a contact with conductance $M\ G_0$ is comprised of M such atoms. Interestingly also some of the multivalent metals do show histograms with a pronounced peak structure with spacings of the order of G_0 [10], see Fig. 1.

For the case of aluminum where the first histogram peak is located around $0.8G_0$, it has been shown, that contacts with this conductance do transmit more than one channel, mostly three channels [11,12]. In this experiment the channel ensemble has been determined by analyzing the nonlinear current-voltage characteristics of superconducting atomic contacts. In contrast to the observations for monovalent metal contacts, each of these channels has a transmission well below one. It has been argued that these findings might be either due to strong disorder in the contact region induced by the particular sample fabrication method that involves thin evaporated films [13] or by the influence of the determination procedure relying on superconductivity. However, additional evidence for not completely open channels is again found in the shot-noise signal of aluminum contacts in the normal state fabricated with the MCB method from bulk aluminum [7]. The fact that more than one channel contributes to the conductance of a single-atom contact is naturally explained by a quantum che-

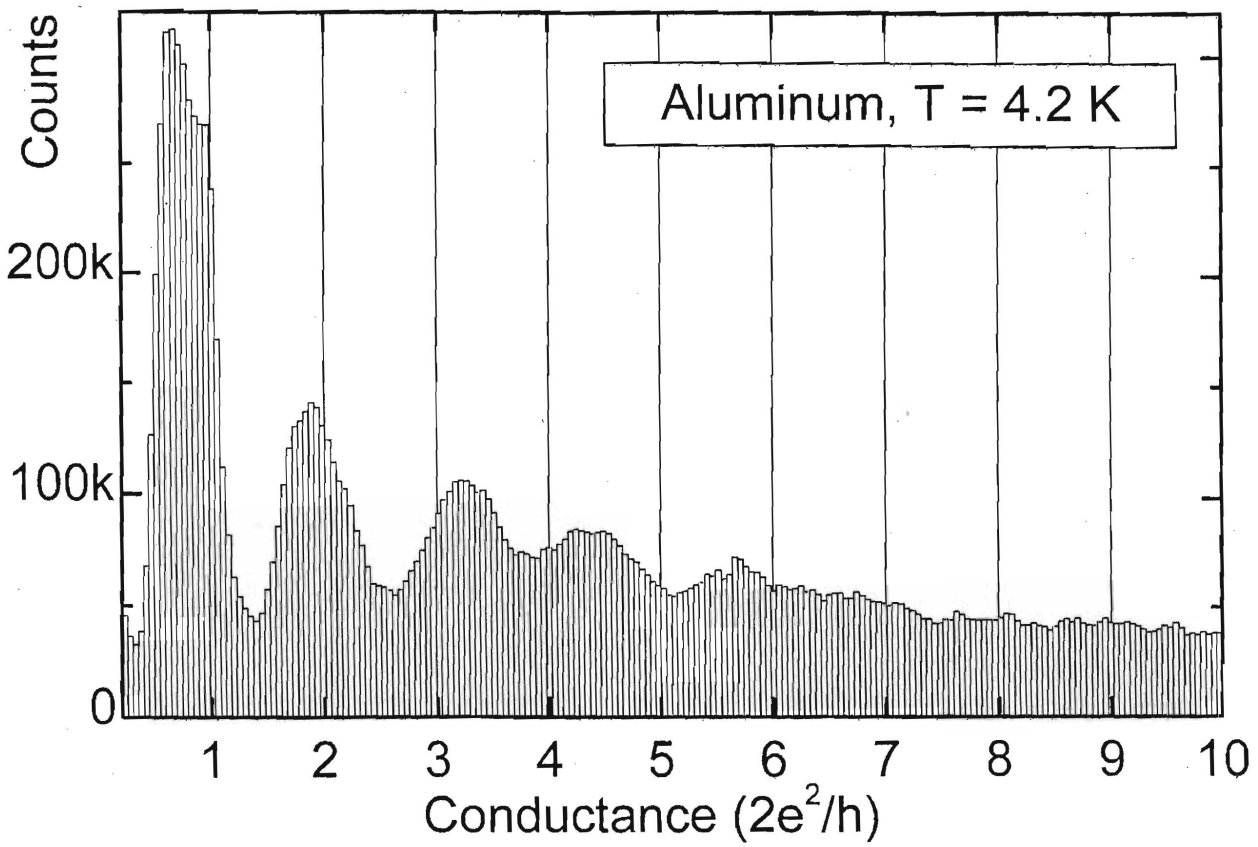

Fig. 1. Conductance histogram constructed from over 30000 individual opening curves for two different samples made of aluminum fabricated by the MCB technique. Each curve was recorded at 4.2 K while stretching contact to break. From [10]

mical model that calculates the transport channel in a tight-binding formalism starting from the valence orbitals of the metal [14,15]. This description implies that the conductance properties of atomic-size contacts are dominated by atomic arrangements. E.g. jumps in the conductance when stretching a contact would be a consequence of a rearrangements of the atoms as suggested by the experiment from Rubio *et al.* [16] who showed that the jumps in the *conductance* appear simultaneously with a jump in the strain force. A possible explanation of the preferred conductance values could thus be the existence of preferred atomic arrangements of the contact. This would imply the appearance of preferred transmission coefficients. However, this interpretation still lacks a complete explanation why the transmissions of the individual channels of a single Al atom add up to a total conductance value close to 1. The latter is evidenced in Fig. 2. The bottom panel of Fig. 2 shows in detail the evolution of $\{\tau_i\}$ when a contact is opened. The upper panel of Fig. 2 shows the evolution of the total transmission $\mathcal{T}$ as obtained from the sum of all individual transmissions. There are several remarkable features in this evolution. First, the abrupt changes in $\mathcal{T}$ correspond generally to a *complete rearrangement* of the transmission set. Second, even during the more continuous evolution on the tilted plateaus the variations of $\mathcal{T}$ arise from changes in *several* of the individual channels. Interestingly the variations of the total conductance are smaller than the variations of the individual τ_i, since some of the τ_i increase while others decrease. Similar results are observed when

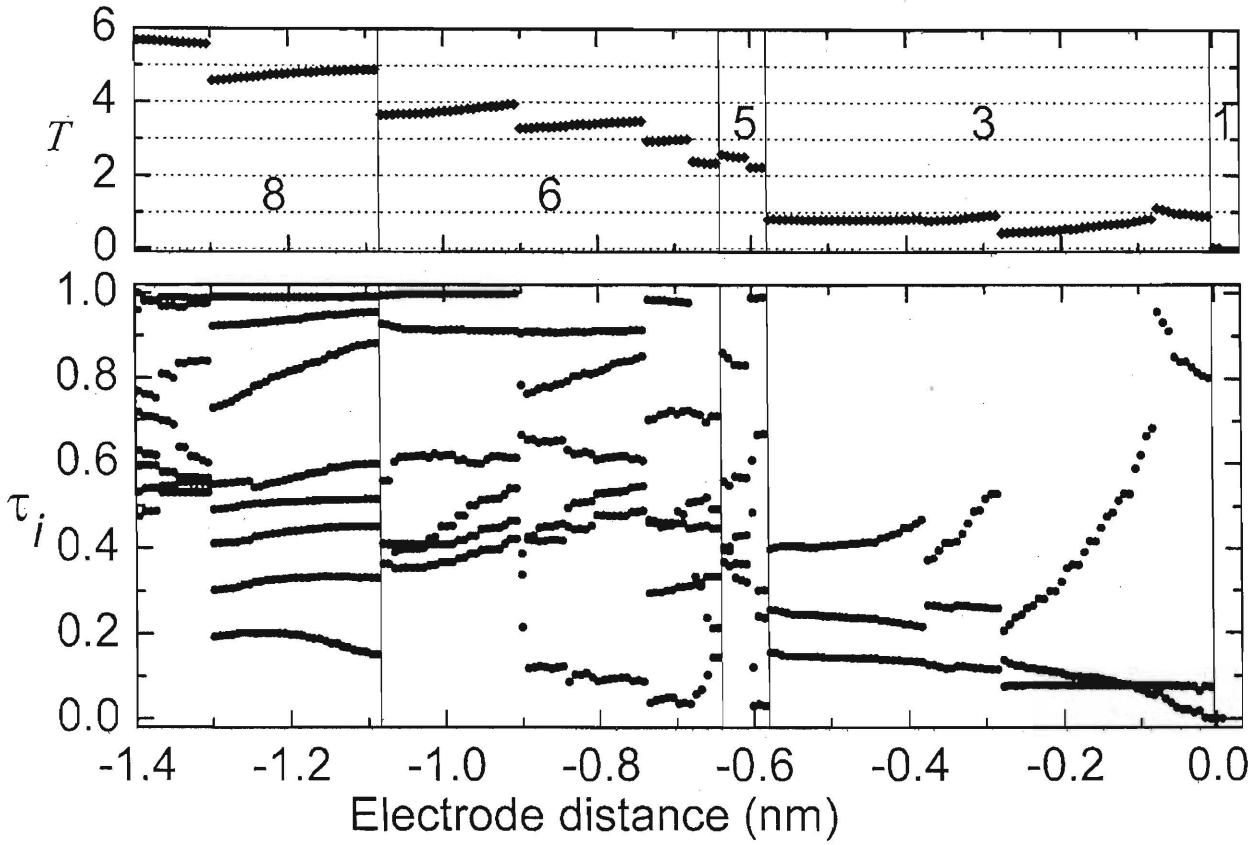

Fig. 2. *Top panel:* total transmission $\mathcal{T}=\sum \tau_i$ as a function of time while opening an aluminum sample at 0.5 pm/s and below 100 mK. *Bottom panel:* evolution of individual transmission coefficients τ_i. The vertical lines correspond to conductance jumps with change of the number of channels. The x-axis scale indicates the approximate variation of the distance between anchors. The origin of the distance axis has been set to the point where the contact breaks and enters the tunnel regime

closing the contacts as shown in Fig. 3. Even within a plateau rearrangements of the $\{\tau_i\}$ occur while the total conductance remains almost unchanged (see e.g. the plateau with $M = 3$ in Fig. 2 or $M = 5$ in Fig. 2. Thus, there seems to be a tendency for the contacts to adopt such contacts that have a preferred value of the total conductance, i.e. the sum of all transmission, regardless of the transmission ensemble itself. The *continuous* evolution of the transmission without abrupt rearrangements can again be explained by a tight binding model which describes the evolution of the LDoS and consequently of the $\{\tau_i\}$ [17]. However, the mechanism giving rise to channel rearrangements without change of G remains unclear.

In what follows we describe the non-self-consistent tight binding calculation, stress the special role of the constriction and present a possible explanation for the observed behavior.

3 Tight-Binding Modelling for Break-Junctions

It is a hallmark of Fermi liquid theory that for low-lying excitations the electron-electron interaction leads only to a renormalization expressed in terms of Fermi

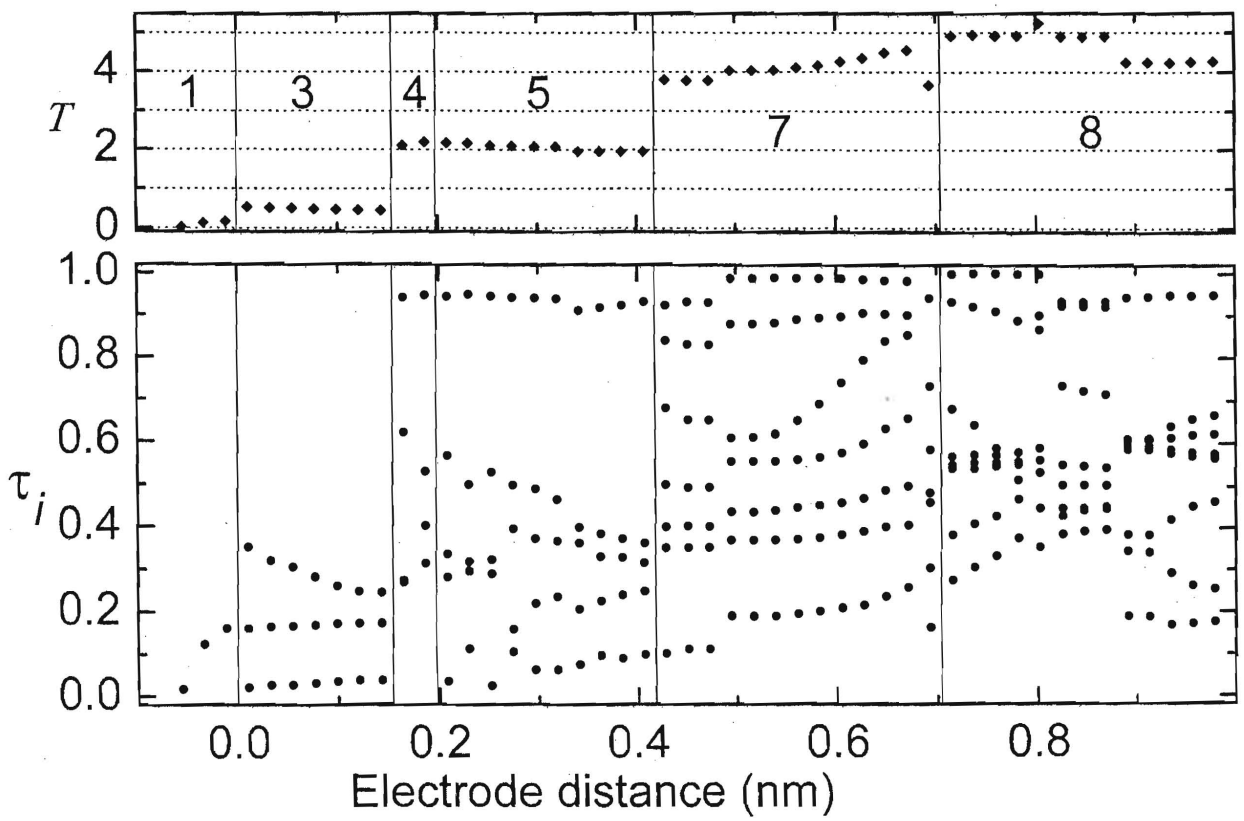

Fig. 3. Same as Fig. 2 when closing the contact at a speed of 1.1 pm/s

liquid parameters. In calculating bulk properties of so-called 'simple' metals - in contrast to e.g. narrow band materials- the electron-electron interaction can safely be neglected altogether. In those cases the band structure and, therefore, the LDoS is easily obtained from a band structure calculation using, e.g., a non-self-consistent tight-binding model of the material under consideration [18,19]. In general the tight binding method aims at replacing the exact many-body Hamiltonian H by a parametrized Hamiltonian matrix in a basis of well localized functions ('atomic orbitals'). The omission of the Coulomb interaction among the electrons leads to a Hamiltonian matrix that does not depend on the distribution of electrons. Consider a usual tight-binding Hamiltonian H_{TB}:

$$H_{TB} = \sum_{\substack{i,\alpha \\ \sigma}} \epsilon_{i\alpha} c^{\dagger}_{i\alpha\sigma} c_{i\alpha\sigma} + \sum_{<i,j>} \sum_{\substack{\alpha,\beta \\ \sigma}} t_{i\alpha,j\beta} c^{\dagger}_{i\alpha\sigma} c_{j\beta\sigma}, \tag{4}$$

where i runs over all the atoms, α, β are band indices and $\sum_{<i,j>}$ is a restricted sum over nearest neighbors only. In the following N will be the total number of atoms and n will denote the number of bands.

The hopping element $t_{i\alpha,j\beta}$ of (4) is obviously equal to $\langle \phi_{i\alpha} | H_{TB} | \phi_{j\beta} \rangle$, where $|\phi_{i\alpha}\rangle = c^{\dagger}_{i\alpha} |0\rangle$. The Slater-Koster two-center approximation approximates this integral in the case of $i \neq j$ by [20,21]

$$t_{i\alpha,j\beta}(\boldsymbol{b}_i - \boldsymbol{b}_j) = \int d^3r \, \tilde{\psi}^*_{i\alpha}(\boldsymbol{r} - \boldsymbol{b}_i) \tilde{H} \tilde{\psi}_{j\beta}(\boldsymbol{r} - \boldsymbol{b}_j), \tag{5}$$

where $\tilde{H}$ is the two-center part of the Hamiltonian H consisting of the kinetic energy operator and the (considered spherically symmetric) part of the single-particle potential on atom i and j located at position $\boldsymbol{b}_i$ and $\boldsymbol{b}_j$. The $\tilde{\psi}_{j\beta}$ are Löwdin orbitals. These hopping elements depend on the magnitude - usually the lattice constant - and the orientation of $\boldsymbol{u}$, determined by the lattice type. In the case where the two atoms are identical, the $t_{i\alpha,j\beta}(\boldsymbol{u})$ can be parameterized by ten independent 'Slater-Koster parameters' usually denoted by $h_{\alpha\beta\gamma}$ where α and β specify the orbital angular momenta (s, p, d), and $\gamma = \sigma, \pi, \delta$ specifies the angular momentum component relative to the vector $\boldsymbol{u}$ connecting atom i and atom j. The relation between the $t_{i\alpha,j\beta}$ of (4) and the Slater Koster parameters is relatively simple for s- and p-like orbitals and fixed distance or lattice constant.

A frequently used method to go beyond this simple tight-binding approach and to include some aspects of the electron-electron interaction for bulk properties is via the local charge neutrality condition (LCNC). The tight-binding Hamiltonian, (4) might give rise to spurious charge transfer resulting in a local charge different from the ionic charge. In a good metal, this net charge is usually screened on a scale -the screening length- smaller than the lattice constant, thereby restoring a uniform charge density. This is modelled by the LCNC by enforcing an electron density that equals on each site the ionic charge. The tight-binding method augmented with the condition of local charge neutrality, which enforces the same occupation on each site has been employed by A. Yeyati [14] and J. C. Cuevas [19,15,17] to obtain the evolution of the channel transmissions in atomic break-junctions when stretching the contacts.

4 A Multi-level Impurity Model

The opening of the quantum point contact just before rupture might be modelled by varying the overlap of the wavefunctions of the atom or atoms in the constriction with its neighbors. According to Harrison [22] a lattice constant dependence can easily be built into the $t_{i\alpha,j\beta}$ to obtain the band structure at different lattice spacings by scaling the Slater-Koster parameters as d^{-2} for the (s, s), (s, p), and (p, p) parameters, where d is the ratio between new and old lattice spacing. Other parameters show a more complex scaling. The (s, d) elements for example scale as $d^{-7/2}$. Harrison's scaling argument might be oversimplified in many instances. In any case the overlap of the wavefunctions and hence the $t_{i\alpha,j\beta}$ have to vanish exponentially for large enough d.

We will now rewrite the tight-binding Hamiltonian in order to stress the central role of the atom(s) in the constriction which will be referred to as the central atom or impurity.

After redistributing the indices i in such a way that $i = 0$ corresponds to the central atom, H_{TB} ofn (4) can be rewritten as:

$$
\begin{aligned}
H_{TB} &\equiv H_B + H_C \\
H_B &= \sum_{\substack{i\neq 0 \\ \alpha,\sigma}} \epsilon_{i\alpha} c^\dagger_{i\alpha\sigma} c_{i\alpha\sigma} + \sum_{\substack{<i,j> \\ i\neq 0, j\neq 0}} \sum_{\substack{\alpha,\beta \\ \sigma}} t_{i\alpha,j\beta} c^\dagger_{i\alpha\sigma} c_{j\beta\sigma} \qquad (6) \\
H_C &= \sum_{m,\sigma} \epsilon_m c^\dagger_{0m\sigma} c_{0m\sigma} \\
&\quad + \sum_{\substack{i=\mathrm{n.N.} \\ \beta}} \sum_{m,\sigma} \left(t_{0m,i\beta} c^\dagger_{0m\sigma} c_{i\beta\sigma} + t_{i\beta,0m} c^\dagger_{i\beta\sigma} c_{0m\sigma} \right).
\end{aligned}
$$

$\sum_{i=\mathrm{n.N.}}$ denotes a sum over the nearest neighbors of the central atom. In order to have H_{TB} hermitian, the hopping elements have to satisfy $t_{i\alpha,j\beta} = t^*_{j\beta,i\alpha}$. This then implies that H_B is an hermitian operator and hence can be diagonalized by a unitary transformation:

$$
\tilde{\mathbf{U}} H_{TB} \tilde{\mathbf{U}}^{-1} = \tilde{\mathbf{U}} H_B \tilde{\mathbf{U}}^{-1} + \tilde{\mathbf{U}} H_C \tilde{\mathbf{U}}^{-1}, \qquad (7)
$$

where $\tilde{U} H_B \tilde{U}^{-1}$ is diagonal in the new basis. With the following transformation of the annihilation and creation operators from the old to the new representation

$$
c_{k\sigma} = \sum_{i\alpha} U^{i\alpha}_k c_{i\alpha,\sigma} \qquad (8)
$$

the hybridization term between the central atom and the leads assumes the following form (for simplicity: $t_{0m,i\beta} \to t_{m,i\beta}$ and $c^\dagger_{0m\sigma} \to d^\dagger_{m\sigma}$):

$$
\begin{aligned}
\sum_{\substack{i=\mathrm{n.N.} \\ \beta,m,\sigma}} t_{m,i\beta} d^\dagger_{m\sigma} c_{i\beta\sigma} &= \sum_{\substack{k,\sigma \\ m}} \sum_{\substack{i=\mathrm{n.N.} \\ \beta}} t_{m,i\beta} d^\dagger_{m\sigma} (U^k_{i\beta})^* c_{k\sigma} \\
&\equiv \sum_{\substack{k,\sigma \\ m}} V^m_k d^\dagger_{m\sigma} c_{k\sigma}, \qquad (9)
\end{aligned}
$$

where V^m_k is given by

$$
V^m_k = \sum_{\substack{i=\mathrm{n.N.} \\ \beta}} t_{m,i\beta} (U^k_{i\beta})^*. \qquad (10)
$$

In this basis the tight-binding Hamiltonian equation (4) can therefore be written as:

$$
\begin{aligned}
H_{TB} &= \sum_{k,\sigma} \epsilon_k c^\dagger_{k\sigma} c_{k\sigma} + \sum_{m,\sigma} \epsilon_m d^\dagger_{m\sigma} d_{m\sigma} \qquad (11) \\
&\quad + \sum_{k,\sigma} \sum_{m} (V^m_k d^\dagger_{m\sigma} c_{k\sigma} + \mathrm{h.c.}).
\end{aligned}
$$

This is nothing but a multi-level impurity model without Coulomb repulsion on the impurity ($U = 0$). In general $t_{i\alpha,j\beta} \neq 0$ for $\alpha \neq \beta$, which is –in parts– a consequence of s-p hybridization. Therefore the resulting model (even for only one local level) is different from the usual $SU(n) \times SU(2)$ Anderson model although several bands are involved.

5 Electronic Density and Static Screening in the Constriction

In the following we will argue that the LCNC breaks down in the constriction and therefore a tight-binding approach together with a local charge neutrality constraint treats the Coulomb interaction in an oversimplified way.

In order to understand how a local charge neutrality constraint can modify the transmission through the constriction we will employ a semiclassical argument to see that the geometric constriction will alter the screening length. In a metallic system a local impurity potential Φ shifts the energy levels locally by an amount Φ. In order to guarantee a spatially uniform Fermi energy E_F throughout the system electrons will have to be redistributed such that the potential generated by the density change $\delta n(\boldsymbol{r})$ according to Poisson's law cancels the impurity potential. Therefore the impurity potential is related to the local electron density via

$$\nabla^2 \Phi(\boldsymbol{r}) = \delta n(\boldsymbol{r})\, e/\epsilon_o \approx D(\boldsymbol{r}, E_F)\, \Phi(\boldsymbol{r})\, e^2/\epsilon_o, \tag{12}$$

where $D(\boldsymbol{r}, E_F)$ is the local density of states and $\Phi \ll E_F$ has been assumed. In spherical coordinates and with open boundary conditions we obtain the Thomas Fermi screening length for the bulk:

$$\lambda_T = \sqrt{\epsilon_o / e^2 D(E_F)}. \tag{13}$$

For aluminum the bulk screening length is roughly $\lambda_T \sim 0.5$ Å. The lattice constant is approximately $a \sim 4$ Å and therefore $\lambda_T \ll a$ for the bulk.

In order to obtain the corresponding screening length in a quantum point contact where the finite boundary conditions will change the screening properties of the electrons, not only (12) in the presence of the new boundary conditions has to be solved. In addition, the Schrödinger equation must be solved to take the effect on the local electron density into account. In standard perturbation theory this would correspond to solving the random phase approximation (RPA) for the chosen geometry.

In the following we consider a simple toy model to simulate the effect of the finite geometry. To this end we model the elongation of the quantum wire in oblate spheroidal coordinates (ζ, η, ϕ). The coordinate surfaces of this system are confocal ellipses and hyperbolas rotated around the minor axis. We will use this set of coordinates since a suitable approximation of the surface of the sample is obtained by having $\eta = \pm\eta_0$ with $0 < \phi < \pi$ and $1 < \zeta < \infty$. The elongation of the quantum wire is then modelled by a decrease in η_0. The minimal possible η_0 is assumed while the wire breaks and should be below a lattice constant. Fig. 4 shows this surface for various η_0. For details of this model and oblate spheroidal coordinates see [23,24]. J. Torres et al have generalized the Landauer-Büttiker formula to a wire with similar geometry [25]. Kassubek *et al.* have used a free-electron model for two- and three-dimensional wires [26]. Imposing hard wall boundary conditions and neglecting Coulomb interaction among the electrons

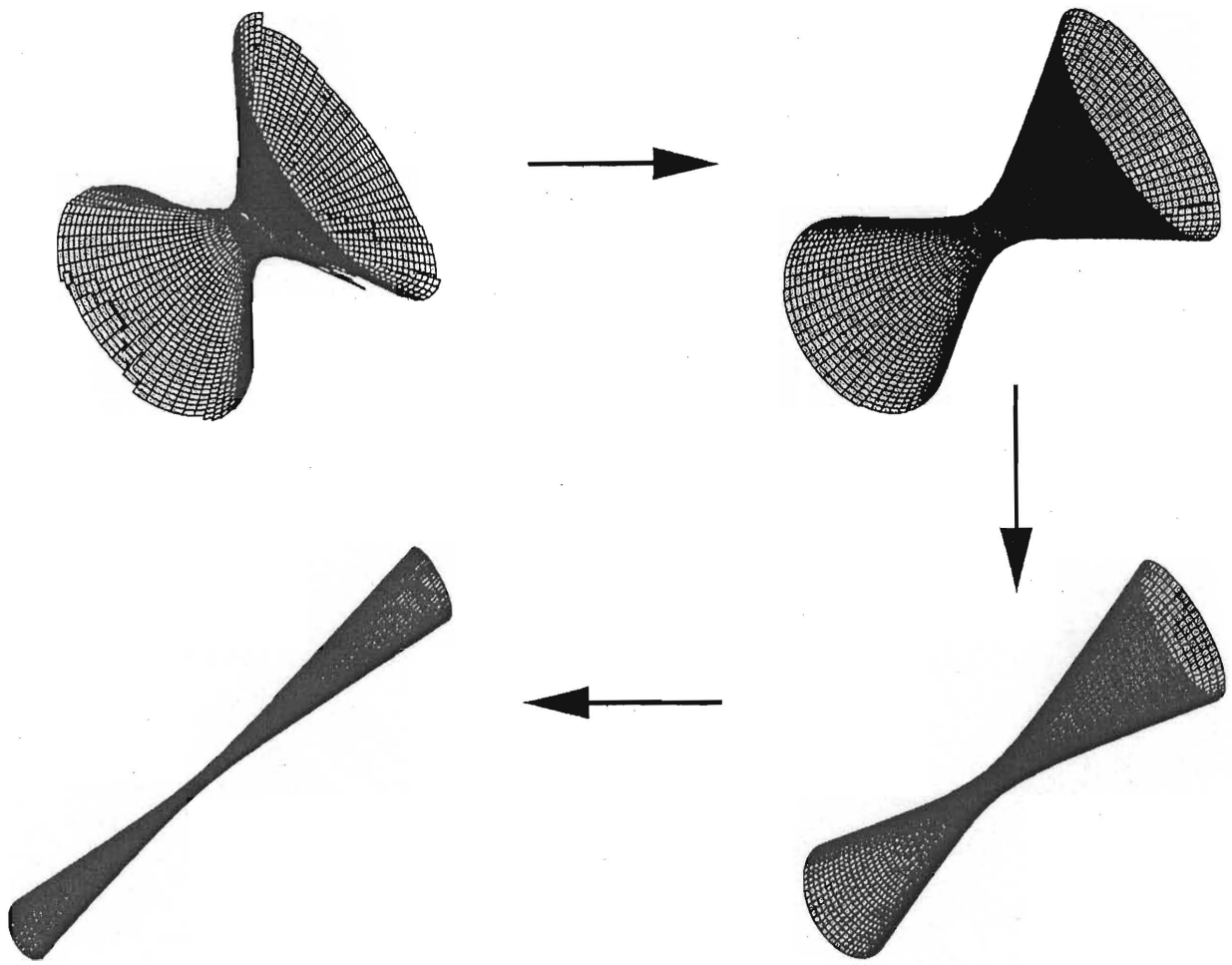

Fig. 4. Modelling the break-junction experiment: While opening the contact the central region of the quantum wire gets thinner until it breaks. In this simple model of the experiment we describe the wire by a surface of constant η_0 in oblate spheroidal coordinates (ζ, η, ϕ) and the opening of the contact by a decrease in η_0. For details, see [23,24]

we solve for the one-particle density. As expected, the increase in kinetic energy leads to a depletion of the density in the constricted region. Figure 5 shows our result for the electron density where we assumed the first 200 eigenstates to be occupied. In the numerical evaluation we chose a cut-off ζ_0 large enough such that the density in the constriction ($\zeta \approx 1$) did not depend on it.

Although we neglected the Coulomb interaction in our toy model, which will try to balance any density fluctuations, it is clear that the competition between kinetic energy and interaction cannot restore a uniform density. LCNC on the contrary enforces a uniform density by assuming that $\lambda_T \ll a$ everywhere. Forcing the system to a constant screening length even in the constriction will of course modify the LDoS at the Fermi energy, $D(E_F)$. This is analogous to fixing the screening length according to $\lambda_T \ll a$, see (13). Consequently the current and hence the conductance will be modified accordingly. In order to prevent this, the Coulomb interaction in the constriction has to be explicitly taken into account in the tight binding Hamiltonian, (4) without resorting to the

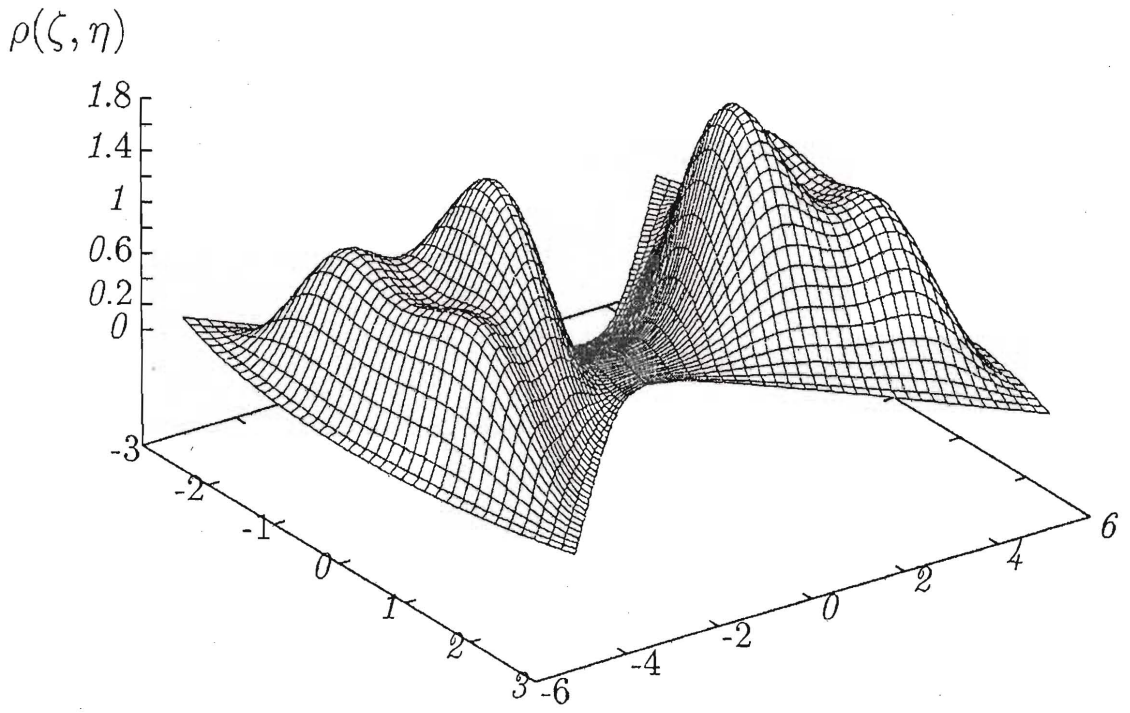

Fig. 5. One-particle density for an opening angle of the point contact corresponding to $\eta_0 = 0.5$. The density does not depend on ϕ due to the symmetry of the chosen hard wall potential. The density in the constriction is depleted in the central region

LCNC. The Hamiltonian we will use to describe the break-junction experiments therefore assumes the form:

$$H = H_{TB} + \frac{1}{2} \sum_{(m,\sigma)\neq(m',\sigma')} U_{m,m'}\, \hat{n}_{m\sigma} \hat{n}_{m'\sigma'}, \tag{14}$$

where we introduced intra- and interlevel Coulomb matrix elements $U_{m,m'}$ in the central region.

In the last section we will derive an approximate sum rule for the total transmission probability $\mathcal{T}$ of the Hamiltonian of (14) with 2 orbitals on the central atom.

6 Conductance in the Strongly Correlated Regime

The current through the quantum point contact described by (14) in the case of symmetric coupling to left and right lead can be related to the LDoS according to [2]

$$I = \frac{e}{\hbar} \sum_{\sigma} \int d\omega \, [f(\omega) - f(\omega + \frac{eV}{\hbar})] \, \mathrm{Im}\, \mathrm{tr}\{\Gamma \cdot \mathcal{G}_\sigma(\omega)\}.$$

Here, $\mathcal{G}_\sigma$ is the local Green function and the lead-to-orbital coupling matrix Γ is given by [2]:

$$\Gamma_{nm} = 2\pi \sum_{k} \rho_k(\epsilon) V_k^n V_k^{m*}, \tag{15}$$

where $\rho_k(\epsilon)$ is the density of states of the leads. The conductance follows immediately:

$$G = \frac{dI}{dV}\Big|_{V=0} = \mathrm{Im}\{\Gamma \cdot \mathcal{G}_\sigma(0)\}. \tag{16}$$

The lattice constant dependence of the elements of Γ is obtained from (10) and Harrison's scaling law as

$$\Gamma_{nm} = 2\pi\rho(0) \sum_{\substack{i=\mathrm{n.N.} \\ \alpha}} t_{m,i\alpha} t_{i\alpha,n} \sim d^{-4}, \tag{17}$$

which is a rather strong lattice constant dependence. Since the ground state of H in (14) is a spin singlet [27], the quantum dot acts for low enough temperatures as a pure potential scatterer for electrons traversing the system, and the following Fermi liquid relations hold [28,24],

$$\Sigma_m''(\omega) = \frac{(\hbar\omega)^2 + (\pi k_B T)^2}{k_B T_K} \qquad \omega, T < T_K \tag{18}$$

$$\int_{-\infty}^{0} d\omega \ \mathrm{tr}\Big\{\frac{\partial\Sigma(\omega)}{\partial\omega} \cdot \mathcal{G}_{d\sigma}(\omega)\Big\} = 0, \tag{19}$$

where T_K is a dynamically low energy scale of the system, analytically given in [29]. The averaged electron number in the dot per spin, $n_{d,\sigma}$, can now be evaluated using the general relation $\frac{d}{d\omega}\ln(\mathcal{G}_d^{-1}) = (1 - \frac{d\Sigma}{d\omega}) \cdot \mathcal{G}_d$ and the Luttinger theorem (19),

$$n_{d\sigma} = \mathrm{Im}\int_{-\infty}^{0} \frac{d\omega}{\pi} \mathrm{tr}\ \mathcal{G}_{d\sigma}(\omega) = \frac{\mathrm{Im}}{\pi}\Big[\mathrm{tr}\{\ln \mathcal{G}_{d\sigma}(\omega)^{-1}\}\Big]_{-\infty}^{0}.$$

It may be re-expressed, using $\mathrm{tr}\ \ln \mathcal{G}_{d\sigma}{}^{-1} = \ln \det \mathcal{G}_{d\sigma}{}^{-1}$, as

$$n_{d\sigma} = \frac{1}{\pi}\mathrm{arccot}\left[\frac{\mathrm{Re\ det}\ \mathcal{G}_{d\sigma}(0)^{-1}}{\mathrm{Im\ det}\ \mathcal{G}_{d\sigma}(0)^{-1}}\right]. \tag{20}$$

The scattering T-matrix of the device, $\Gamma \cdot \mathcal{G}_{d\sigma}$, which for symmetric coupling to left/right lead completely determines the conductance G. Using the Fermi liquid property equation (18) together with the Dyson equation relating $\mathcal{G}_{d\sigma}$ and $\Sigma_\sigma(\omega)$ and (20), we obtain at the Fermi energy ($\omega = 0$, $T \ll T_K$) for $n = 2$,

$$\mathrm{Im\ tr}\ (\Gamma \cdot \mathcal{G}_\sigma(0)) = \sin^2(\pi n_{d\sigma}) + \sin(2\pi n_{d\sigma}) \frac{\mathrm{Re}[\det(i\Gamma - \Sigma'(0))]}{\Gamma_{11}(\varepsilon_{d,2} + \Sigma_{22}'(0)) + \Gamma_{22}(\varepsilon_{d,1} + \Sigma_{11}'(0))}. \tag{21}$$

This is an exact result, valid for arbitrary microscopic parameters Γ_{nm}, ε_m and $U_{m,m'}$. It is the generalization of the well-known unitarity rule of the single-level Anderson impurity problem to the case of several impurity levels [30]. Having

at least one of the local levels significantly below the Fermi level ($\varepsilon_{m=1} < 0$, $|\varepsilon_{m=1}|/\Gamma_{nm} > 1$) and the Coulomb repulsion large enough ($U_{m,m'}/\Gamma_{nn'} \gg 1$) to enforce $n_{d\sigma} \approx 1/2$ we obtain a conductance close to the conductance unit. This resembles the observed behavior. The condition $U_{m,m'}/\Gamma_{nn'} \gg 1$ can be met through the decrease in the hopping amplitude while opening the contact. This situation is analogous to the situation in narrow band materials where the small band width leads to a strongly correlated state. Provided the wire does not break and the temperature is well below the low energy scale T_K, which depends exponentially on the entries of the coupling matrix, it seems that we will always reach this regime while elongating the wire according to (17).

Acknowledgments

It is a pleasure to acknowledge stimulating discussions with F. Evers, H. v. Löhneysen, A. Mildenberger, and J. Paaske. Finally, we have enjoyed fruitful interaction with D. Averin, J.C. Cuevas and A. Levy Yeyati, and we thank them for providing us with their respective computer codes. The experiments have been performed in collaboration with C. Urbina at the CEA Saclay, France. We thank J.M. van Ruitenbeek for the allowance to reproduce his data. This work was partially supported by the Center for Functional Nanostructures (CFN) and Sonderforschungsbereiche SFB513 and SFB195 of the Deutsche Forschungsgemeinschaft.

References

1. Y.V. Sharvin. Sov. Phys. JETP **21**, 655 (1965)
2. Y. Meir, N. Wingreen. Phys. Rev. Lett. **68**, 2512 (1992)
3. J.M. van Ruitenbeek. In *Mesoscopic Electron Transport*, eds. L.L. Sohn, L.P. Kouwenhoven, G. Schön (Kluwer Academic, Dordrecht, 1997), pp. 549–579; and references therein
4. L. Olesen, E. Laegsgaard, I. Stensgaard, F. Besenbacher, J. Schiøtz, P. Stoltze, K. Jacobsen, J. Nørskov. Phys. Rev. Lett. **72**, 2251 (1994)
5. J.L. Costa-Krämer, N.P. García-Mochales, P.A. Serena. Surface Science **342**, L1144 (1995)
6. J.M. Krans, J.M. van Ruitenbeek, V.V. Fisun, I.K. Yanson, L.J. de Jongh. Nature **375**, 767 (1995)
7. H. van den Brom, J.M. van Ruitenbeek. Phys. Rev. Lett. **82**, 1530 (1999)
8. B. Ludoph, M.H. Devoret, D. Esteve, C. Urbina, J.M. van Ruitenbeek. Phys. Rev. Lett. **82**, 1530 (1999)
9. B. Ludoph, J.M. van Ruitenbeek. Phys. Rev. B **59**, 12290 (1999)
10. A. Yanson, J.M. van Ruitenbeek. Phys. Rev. Lett. **79**, 2157 (1997)
11. E. Scheer, P. Joyez, D. Esteve, C. Urbina, M. Devoret. Phys. Rev. Lett. **78**, 3535 (1997)
12. E. Scheer, N. Agraït, J. Cuevas, A. Yeyati, B. Ludoph, A. Martin-Rodero, G. Bollinger, J.M. van Ruitenbeek, C. Urbina. Nature **394**, 154 (1998)
13. J.M. van Ruitenbeek, A. Alvarez, I. Piñeyro, C. Grahmann, P. Joyez, M.H. Devoret, D. Esteve, C. Urbina. Rev. Sci. Inst. **67**, 108 (1996); and references therein

14. A.L. Yeyati, A. Martin-Rodero, F. Flores. Phys. Rev. B. **56**, 10369 (1997)
15. J. Cuevas, A. Yeyati, A. Martin-Rodero. Phys. Rev. Lett. **80**, 1066 (1997)
16. G. Rubio, N. Agraït, S. Vieira. Phys. Rev. Lett. **76**, 2302 (1996)
17. J. Cuevas, A. Yeyati, A. Martin-Rodero, G. Bollinger, C. Untiedt, N. Agraït. Phys. Rev. Lett. **81**, 2990 (1998)
18. C. Goringe, D. Bowler, E. Hernández. Rep. Prog. Phys. **60**, 1447 (1997)
19. J. Cuevas, A. Martin-Rodero, A. Yeyati. Phys. Rev. B. **54**, 7366 (1996)
20. P. Slater, G. Koster. Phys. Rev. **94**, 1498 (1954)
21. D. Papaconstantopoulos. *Handbook of the Band Structure of Elemental Solids* (Plenum Press, New York, 1986)
22. W. Harrison. *Electronic Structure and the Properties of Solids* (W.H. Freeman and Co., 1980)
23. M. Abramowitz, A. Stegun, eds. *Handbook of Mathematical Functions* (Dover Publications, Inc., New York, 1965)
24. S. Kirchner. Shaker, Aachen (2002), ISBN 3-8322-0183-1.
25. J. Torres, J. Sáenz. Phys. Rev. Lett. **77**, 2245 (1996)
26. F. Kassubek, C.A. Stafford, H. Grabert. Phys. Rev. B **59**, 7560 (1999)
27. A. C. Hewson. *The Kondo Problem to Heavy Fermions* (Cambridge University Press, Cambridge, 1993)
28. A. Yoshimori, A. Zawadowski. J. Phys. C **15**, 5241 (1982)
29. J. Kroha, S. Kirchner, G. Sellier, P. Wölfle, D. Ehm, F. Reinert, S. Hüfner, C. Geibel. to appear in Physica B (2003)
30. S. Kirchner, J. Kroha, E. Scheer. In *Kondo Effect and Dephasing in Low-Dimensional Metallic Systems*, eds. V. Chandrasekhar, C.V. Haesendonck, A. Zawadowski (Kluwer Academic Publishers, Dordrecht, 2001)